



www.ericjournal.iitg.ac.th

An Experimental Investigation of Hydrodynamics and Heat Transfer Characteristics of Biomass Blending in a Pressurized Circulating Fluidized Bed

P. Kalita^{*1}, U.K. Saha[#] and P. Mahanta[#]

Abstract – In the present investigation, the effects of blending of biomass in sand, superficial velocity and operating pressure on bed hydrodynamics and heat transfer in a pressurized circulating fluidized bed have been studied. Experiments have been conducted at four different percentage blending of biomass such as 2.5%, 7.5%, 15% and 20% in sand and with two different weight composition ratios. All the above studies have been made at two different superficial velocities of 5 and 7 m/s and at three different operating pressures such as 1, 3 and 5 bar. The sand and biomass particle sizes used for the study are 309 μm and 407 μm , respectively. Results show that, with the increase in operating pressure, the bed voidage decreases. The axial heat transfer coefficient increases from the bottom to the top of heat transfer probe with the increase in operating pressure. The radial variation of heat transfer coefficient decreases from the wall to the core of the heat transfer probe. The heat transfer coefficient is also found to be increasing with the increase in % blending of sawdust in sand. The overall uncertainty in calculating heat transfer coefficient is found to be 3.90%.

Keywords – Circulating fluidized bed, heat transfer coefficient, pressure, suspension density, voidage

1. INTRODUCTION

Circulating fluidized bed (CFB) technology is one of the most promising technologies used in various chemical and power industries because of its unique in-situ capture of SO_2 and NO_x , and higher thermal efficiency. Pressurized circulating fluidized bed (PCFB) is the second generation technology which is still in the pilot scale level. Extensive research on the design and various parameters influencing the performance of a PCFB is in progress both in industrial and academic level because of its unique advantages such as compactness, fuel flexibility and higher efficiency apart from in-situ capture of SO_2 and NO_x [1]–[3]. The PCFB unit in general, consists of a riser, a cyclone separator, a return leg called downcomer, a loop seal and a feeding system. The performance of a PCFB unit is influenced by a number of factors, including superficial velocity, solid circulation rate, solid inventory, and particle size distribution [1]–[3]. The change of any of these parameters influences the bed hydrodynamics such as bed voidage, suspension density etc. and this causes a change in the heat transfer along the bed height. Till date, researchers have reviewed the bed hydrodynamics and heat transfer characteristics at atmospheric conditions only [3]–[6]. Very limited research information has been reported on the effect of various parameters and blending of biomass in sand in a PCFB. Some of the previous work related to the hydrodynamic and heat

transfer study on CFB is summarized in the following subsections.

Gupta and Nag [1] reported that, with the increase in superficial velocity, the bed voidage increases in the bottom portion and decreases in the top region as more solids are lifted up due to more drag force in a PCFB. The concentration of sand particles is more in the riser column for higher bed inventory, and hence, the bed voidage is lower. The local voidage, and the gas and solid velocities change continuously from the axis to the wall as reported by Hartge *et al.*, Horio *et al.*, Li *et al.* and Yates [7]–[10]. The voidage is highest along the axis of the riser column and lowest in the wall which is observed by Basu, Li *et al.*, and Tang and Engstrom [3], [9], [11]. The radial voidage distribution is much flatter in the upper section of the bed, as well as at lower circulation rates. In case of fast fluidized beds, there is a gas-solid boundary layer, where the solid generally moves downward. This is investigated by Tang and Engstrom, and Schaub, [11], [12] for both in large commercial boilers as well as in laboratory units. Yue *et al.*, [13] suggested that by changing the bed inventory, one can influence the suspension density. The suspension density along the height of a CFB boiler varies exponentially as it does in the freeboard region of a bubbling fluidized bed [14], [15]. However, Andersson and Leckner, [16] and Brereton and Stromberg [17] found that the profile to be better represented by a power-law equation. Yates [18] reviewed the effect of pressure and temperature on fluidized bed and emphasized that more effort needs to be devoted to CFB's as there are many gaps in understanding the flow regime that exist in these system. Wu *et al.*, [19] and Ebert *et al.*, [20] suggested that, except for a very dilute bed, the superficial gas velocity does not have any great influence on the heat transfer coefficient. It is a result of a relatively low contribution of the gas convection

^{*}Centre for Energy, Indian Institute of Technology Guwahati, Guwahati –781039, Assam, India.

[#]Department of Mechanical Engineering, Indian Institute of Technology Guwahati, Guwahati – 781039, Assam, India.

¹Corresponding author; Tel: +913612583127, Fax: +913612690762
E-mail: pankajk@iitg.ernet.in

component. In some situations, the heat transfer coefficient at constant circulation rate even decreases with the increase of superficial velocity due to the resulting decrease in the suspension density [20]-[22]. Divilio and Boyd [23] show a major effect of superficial velocity but a minor effect of suspension density on the heat flux. Gupta and Nag [1], Basu [3], Basu and Nag [4], Basu and Nag [5] and Grace [6] suggested that, the heat-transfer coefficient in a CFB riser increases from the bottom to the top and is influenced by a number of factors, including air flow, solid circulation rate, solid inventory, and particle size distribution. Basu [3] emphasized that the major effect of these parameters on the heat transfer is due to their influence on the suspension density. Glicksman [24] studied the effect of heat transfer coefficient and its dependency on suspension density. It is concluded that, the heat transfer coefficient is found to vary as square root of the cross-section average suspension density. Divilio and Boyd [23] presented an overview of the effect of suspension density on the heat transfer using the data from the laboratory, pilot plants, and operating plants. They observed that, the suspension density varies with the height of the riser. As the combustor gets taller, the solid suspension density decreases further, resulting in lower heat transfer coefficients. Gupta and Nag [1], studied the bed to wall heat transfer behavior in a 37.5 mm ID and 1940 mm height PCFB riser where the heat transfer coefficient was found increasing with an increasing operating pressure as well as with an increase in gas superficial velocity. It was also observed that, with the increase in pressure, the bed voidage increased in the bottom zone of the riser and decreased in the top zone, thereby increasing the suspension density at the top zone. Although much work has been done on the investigation of bed voidage profile, solid circulation rate and heat transfer at varied system pressure both in bubbling and circulating fluidized bed under atmospheric and pressurized conditions, there is no specific information about the investigation of hydrodynamics and heat transfer at varied percentage mixing of biomass in sand in a PCFB. The only information found at the time of writing the paper is that, in the case of bubbling fluidized bed 12% biomass blending in sand is found to be optimum for maximum heat transfer and proper gasification, which is reported in the book written by Oka *et al.* [25]. In the present investigation, the effects of blending of biomass in sand, superficial velocity and operating pressure on bed hydrodynamics and heat transfer in a pressurized circulating fluidized bed has been studied.

2. MATERIALS AND METHOD

2.1 Setup Description

The schematic diagram of the pressurized circulating fluidized bed (PCFB) setup is shown in Figure 1. The PCFB unit comprises of a riser, a transparent downcomer, and a cyclone separator. The riser is made of stainless steel of ID 54 mm and height of 2000 mm.

Air is supplied to the CFB unit through the bottom of the riser by a high pressure centrifugal blower and a compressor. The air flow rate is measured by a standard orifice meter (BS 1042) and is regulated by an air control valve and a bypass arrangement. The air passes through a porous distributor plate (straight hole) of 16.8% opening area which is fixed at the bottom of the riser column. The entrained solids goes out of the riser are recovered in a cyclone separator and are then sent to the bottom of the riser column through a transparent return leg of ID 24.5 mm. Static pressures and hence voidage were measured along the riser height at 6 (six) different locations such as 120 mm, 192.5 mm, 370 mm, 495 mm, 970 mm and 1570 mm above the distributor plate. Suspension densities at those points were also calculated. Fine wire mesh (200 μm) and cigarette filters are used at the pressure tapping ends to minimize the pressure fluctuations and to avoid the escape of sand particles from the column. Pressure drops are measured with U-tube water filled manometer fabricated for this purpose.

2.2 Heat Transfer Probe

The heat transfer probe of height 500 mm is located at a height of 1300 mm above the distributor plate *i.e.* at the upper splash region of the riser. The schematic of the heat transfer probe is presented in the Figure 2. Necessary thermocouples are facilitated to measure the surface and bed temperatures. The locations of the thermocouples from the distributor plate are 1400, 1500, 1600, 1700 and 1800 mm. Besides, thermocouples are also installed to measure the radial temperature variations in the bed at d/D of 0.2, 0.3, 0.4, 0.6 and 0.8 (Figure 3). A heater coil (rated 1000 Watt and resistance 46 Ohms) of the required length is wrapped uniformly around the probe. Adequate electrical and thermal insulation are also provided. Mica sheet of 1 mm thickness is used as electrical insulation over which heater coil. For thermal insulation, ceramic wool and ceramic rope is used around the probe. The axial heat loss by conduction are also prevented by providing ceramic wool insulation in between the joints. Both surface and bed temperatures are measured with chromal-alumal thermocouples and these have been calibrated before use. Agilent 34972 LXI data acquisition/ switch unit is used for measurement and record of temperature.

2.3 Experimental Procedure

A measured quantity of inventory is fed into the unit through the top of the cyclone separator and rests on the ball valve of the transparent return leg (downcomer) till the valve open. Heating of test section was done by a heater coil-auto transformer assembly. The heat transfer probe is heated by providing a known heat flux before the start of experiment. The thermocouples meant for the measurement of bed and wall temperatures are connected to a data acquisition system. Pressure drop along the riser were measured by using a U-tube water manometer. High precision pressure gauge (Swegelok

make) is used for the measurement of the compressor delivery pressure. Blower delivery air flow is controlled by a gate valve installed along the flow, and the flow rate is calculated by measuring the orifice pressure drop (D and $D/2$ tapings) in the U-tube water manometer. Finally, the superficial velocity is calculated by using the measured orifice pressure drop. In each experiment, controlled amount of air is supplied from the blower at a required superficial velocity to the CFB loop (experimental setup). Compressed air is supplied from the compressor at a required pressure to the riser bottom. For each operating condition, about 60 minutes time is required to attain the thermal and hydrodynamic equilibrium. For thermal equilibrium, temperature rise is monitored, and for hydrodynamic equilibrium, circulation rate is monitored. Once the equilibrium condition is reached, experimental data such as temperature, pressure drop and circulation rate are recorded in a data sheet for further analysis. Same procedure is followed with every change in operating parameters. In the experiment, the time taken to accumulate a fixed quantity of solids is measured by closing the ball valve located at the return leg. Stop

watch is used to measure the time of accumulation and the solid accumulation is observed at the graduated scale located just above the ball valve. Experiments were performed at a constant heat flux of 830 W/m^2 and at two different superficial velocities such as 5 and 7 m/s. In each superficial velocity, experiments were conducted at three different system pressures of 1, 3 and 5 bar. The axial variation of heat transfer coefficient with four proportions blending of sawdust in sand such as 2.5%, 7.5%, 15% and 20% have also been studied and compared. Comparisons were also made at two different sets of weight composition ratios one of which is weight composition of sawdust with 400 gm sand and the other is weight composition of sawdust with 600 gm of sand. The percentage blending of sawdust is kept constant irrespective of weight compositions. Average particle size of sawdust used for the experiment is calculated to be $407 \mu\text{m}$. Finally, bed hydrodynamics (bed voidage, suspension density and solid circulation rate) and heat transfer characteristics (axial and radial) were investigated. All the experiments were repeated thrice in order to establish the repeatability.

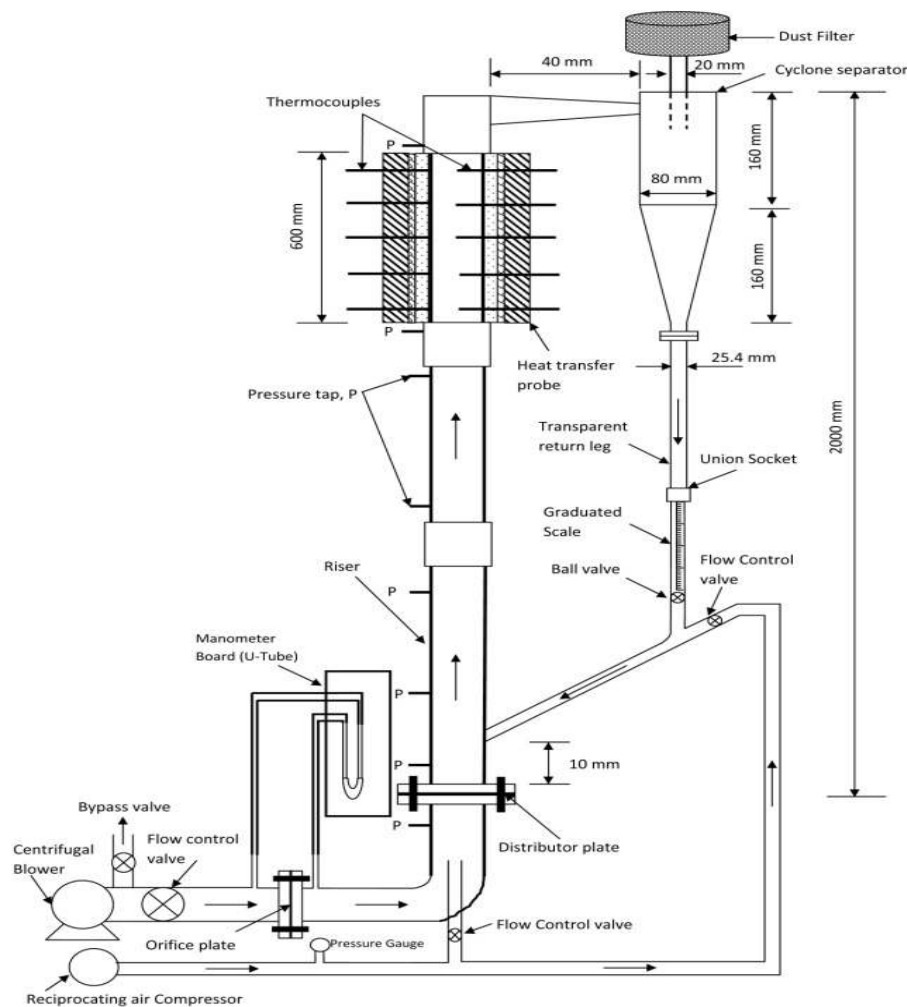


Fig. 1. Schematic of experimental setup.

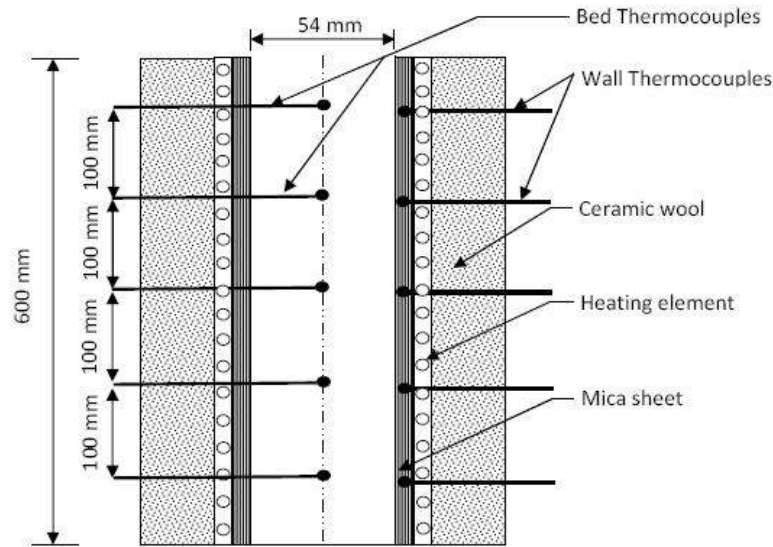


Fig. 2. Schematic of heat transfer probe.

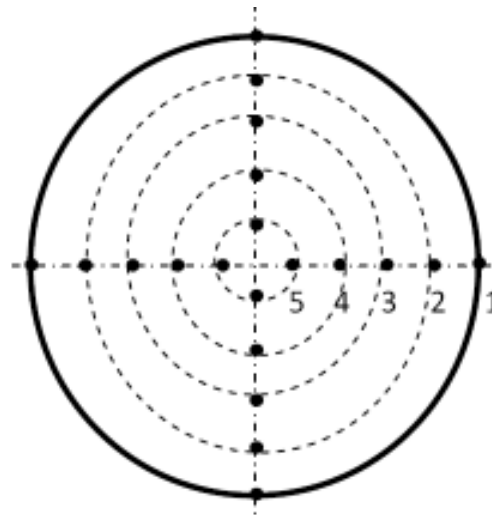


Fig. 3. Location of thermocouples for radial temperature measurement.

2.4 Working Formula

For the axial probe, the wall-to-bed heat transfer coefficient is estimated from the measured local surface to bed temperatures as given below

$$h_i = \frac{q}{A_{\text{htp}}(T_{\text{bs}} - T_{\text{bi}})} = \frac{V \times I}{A_{\text{htp}}(T_{\text{bs}} - T_{\text{bi}})} \quad (1)$$

where i , represents any location along the riser height and A_{htp} , is the heat transfer probe surface area. T_{bs} and T_{bi} are bulk surface temperatures and bed temperatures, respectively.

The *suspension density* of the bed (ρ_{sus}) can be evaluated by the equation (Kunni and Levenspiel [15])

$$\rho_{\text{sus}} = \rho_s (1 - \varepsilon) + \varepsilon \rho_g \quad (2)$$

where voidage (ε) is defined as the volume fraction of the bed occupied by air bubbles, and ρ_g is the density of air in kg/m^3 .

Voidage (ε) may be calculated by using the following expression,

$$\varepsilon = 1 - \frac{10 \times \Delta h}{\rho_s \times L_m} \quad (3)$$

where Δh is the difference of height in manometric fluid measured in cm of water column, L_m is the difference between two consecutive pressure taps across which pressure drops, and ρ_s is the density of sand in kg/m^3 .

Solid circulation rate or solid mass flux (G_s) is given by,

$$G_s = \frac{\rho_s \times L_a \times A_D \times (1 - \varepsilon_{\text{mf}})}{A_B t} \quad (4)$$

where A_B , A_D , G_s , L_a , t , and ϵ_{mf} are cross sectional area of the bed in m², cross sectional area of downcomer in m², solid circulation rate in kg.m⁻².s⁻¹, solid accumulation height in m, time to accumulate particular height after closing ball valve in sec and bed voidage at minimum fluidization respectively.

3. RESULTS AND DISCUSSION

Figures 4 and 5 present the variation and comparison of bed voidage at operating pressures 1 and 5 bar, respectively. The comparisons were made at two

different weight composition ratios and at a superficial velocity of 5 m/s. In these conditions percentage blending of biomass is maintained at 15%. As observed, the bed voidage is first decreases and then increases, before it decreases at the exit of the riser which may be better represented by S-shaped bed voidage profile. With the increase of pressure, the bed voidage is found to decrease at the exit of the riser. This may be due to the increase in concentration of particles at the riser exit. This is observed to be more in the case of weight composition ratio (B/S) of 90:600.

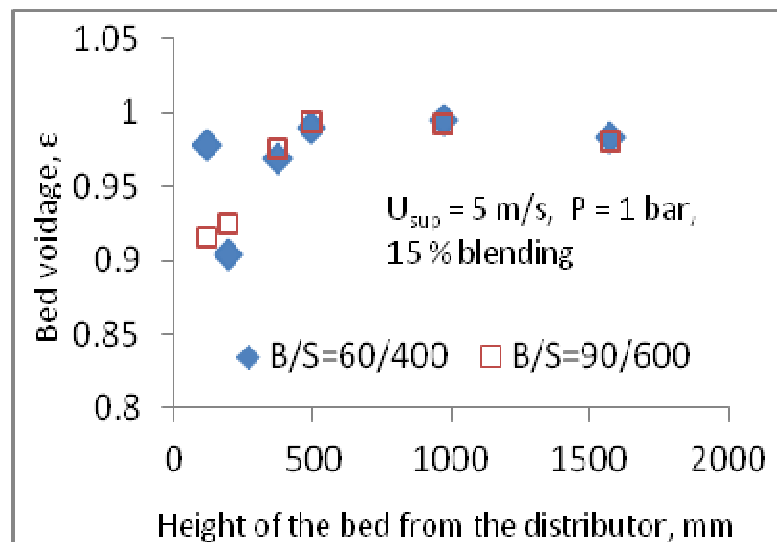


Fig. 4. Variation of bed voidage along the height of the riser at P = 1 bar.

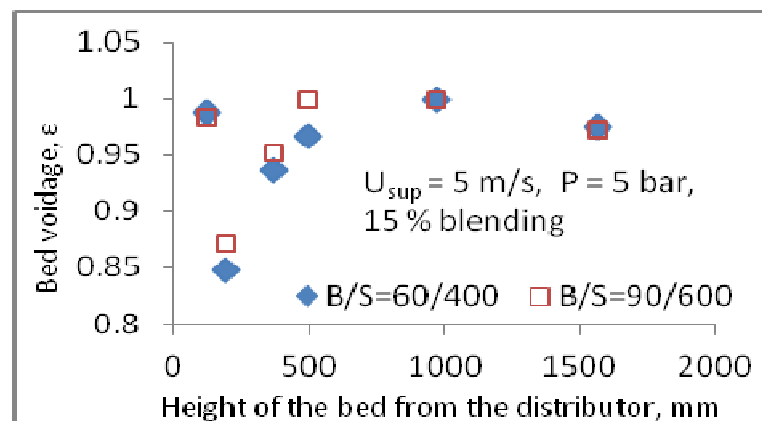


Fig. 5. Variation of bed voidage along the height of the riser at P = 5 bar.

Figures 6 through 13 present the variation of heat transfer coefficient at a height of 1.6 m from the distributor plate at 2.5%, 7.5%, 15% and 20% blending of sawdust in sand. The comparisons were made at two different weight composition ratios and at two different superficial velocities of 5 and 7 m/s. From these figures, it has been observed that, the heat transfer coefficient increases with the increase in operating pressures. At

superficial velocity of 5 m/s, the heat transfer coefficient is found to be higher (120-135 W/m²-K) at 7.5% blending (Figure 7) with weight composition ratio 30 gm: 400 gm as compared to the other three percentage blending. At superficial velocity of 7 m/s, the heat transfer coefficient is found to be higher (between 120-130 W/m²-K) at 15% blending (Figure 12) with weight composition ratio (B/S) of 90 gm:600

gm as compared to the other three percentage blending. The heat transfer coefficient is found to be lowest (90-105 W/m²-K) at 20% biomass blending (Figures 9 and 13) among the other blending at both the superficial velocities *i.e.* at 5 and 7 m/s. This may be due to the

lowest solid circulation rate observed in both the cases as compared to the other percentage blending. The values of the solid circulation rate at the superficial velocities of 5 and 7 m/s and four different percentage blending is shown in the Table 1.

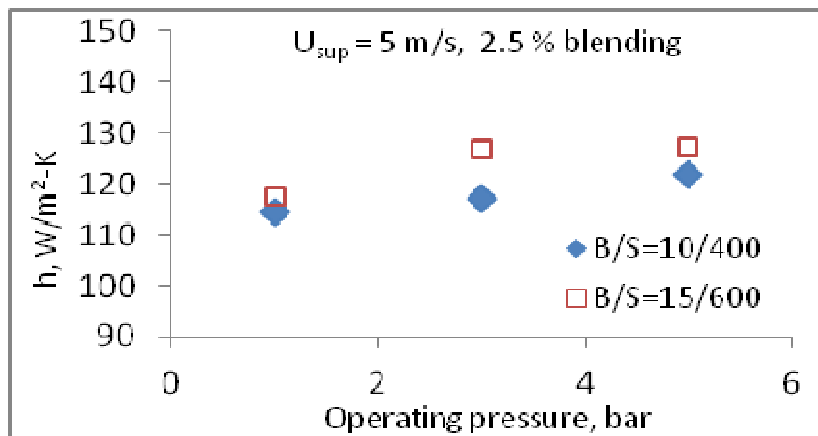


Fig. 6. Variation of heat transfer coefficient at $U_{sup} = 5$ m/s and at 2.5% blending.

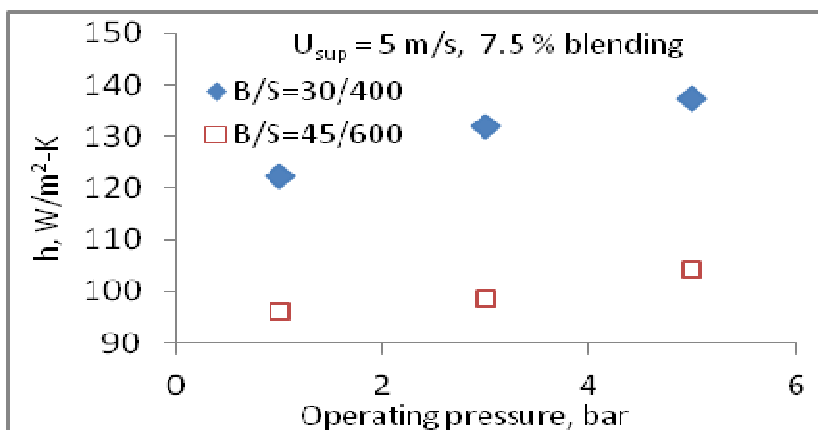


Fig. 7. Variation of heat transfer coefficient at $U_{sup} = 5$ m/s and at 7.5% blending.

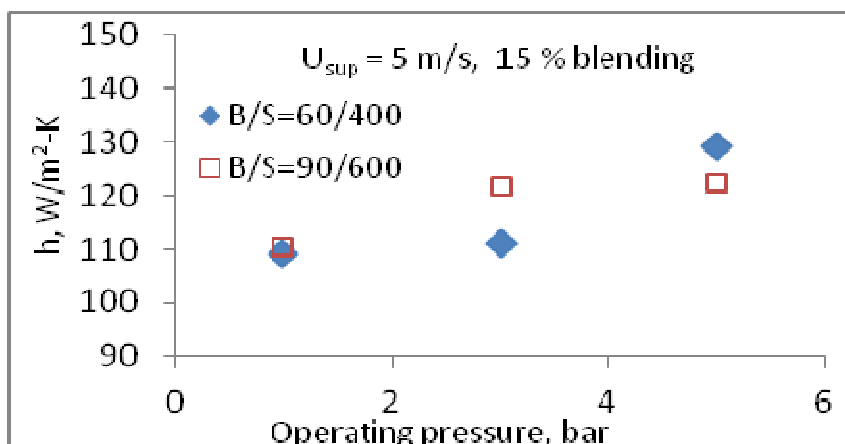


Fig. 8. Variation of heat transfer coefficient at $U_{sup} = 5$ m/s and at 15% blending.

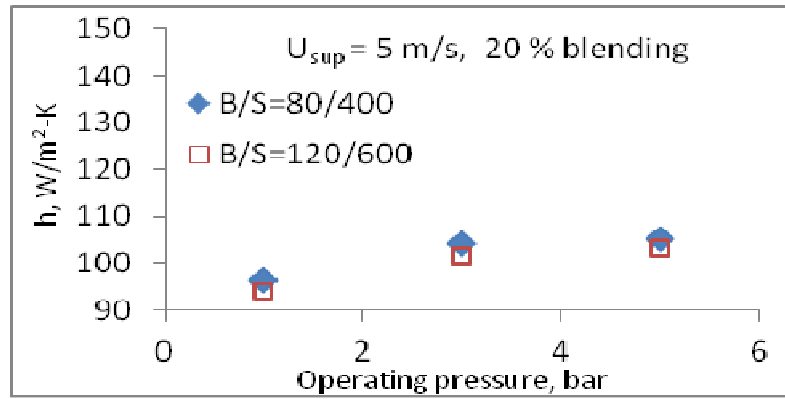


Fig. 9. Variation of heat transfer coefficient at U_{sup} = 5 m/s and at 20% blending.

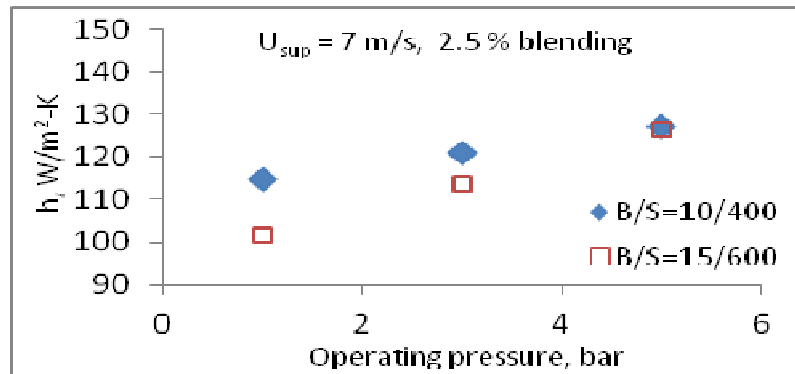


Fig. 10. Variation of heat transfer coefficient at U_{sup} = 7 m/s and at 2.5% blending.

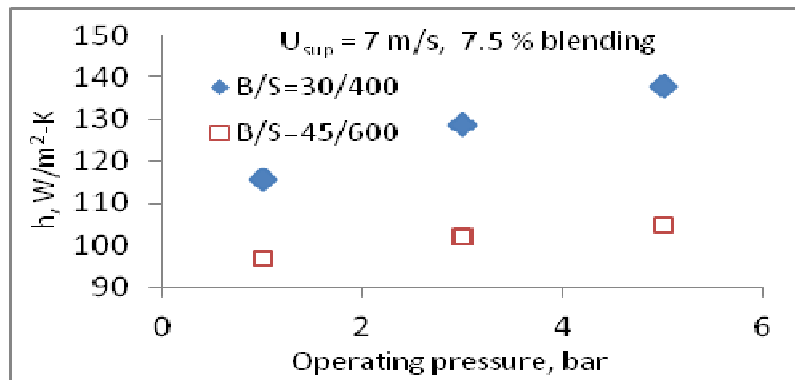


Fig. 11. Variation of heat transfer coefficient at U_{sup} = 7 m/s and at 7.5% blending.

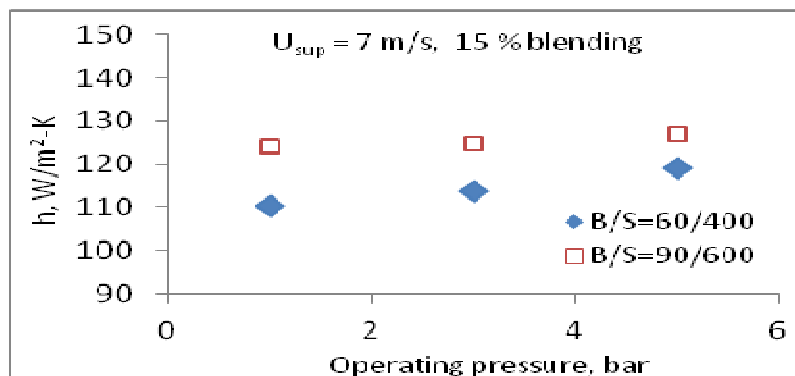


Fig. 12. Variation of heat transfer coefficient at U_{sup} = 7 m/s and at 15% blending.

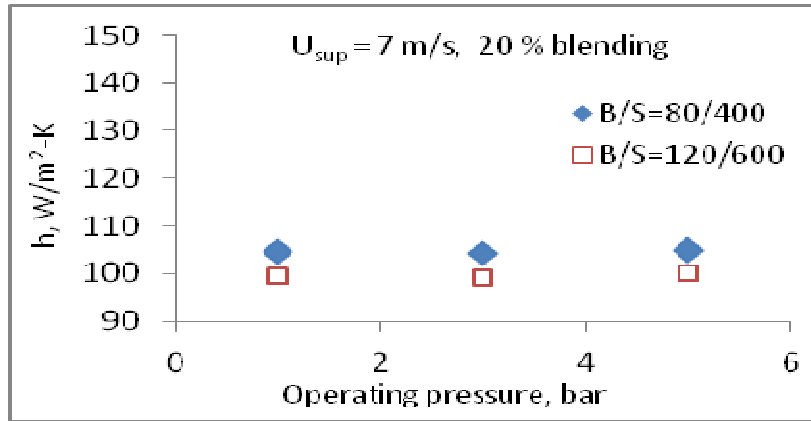


Fig. 13. Variation of heat transfer coefficient at $U_{sup} = 7$ m/s and at 20% blending.

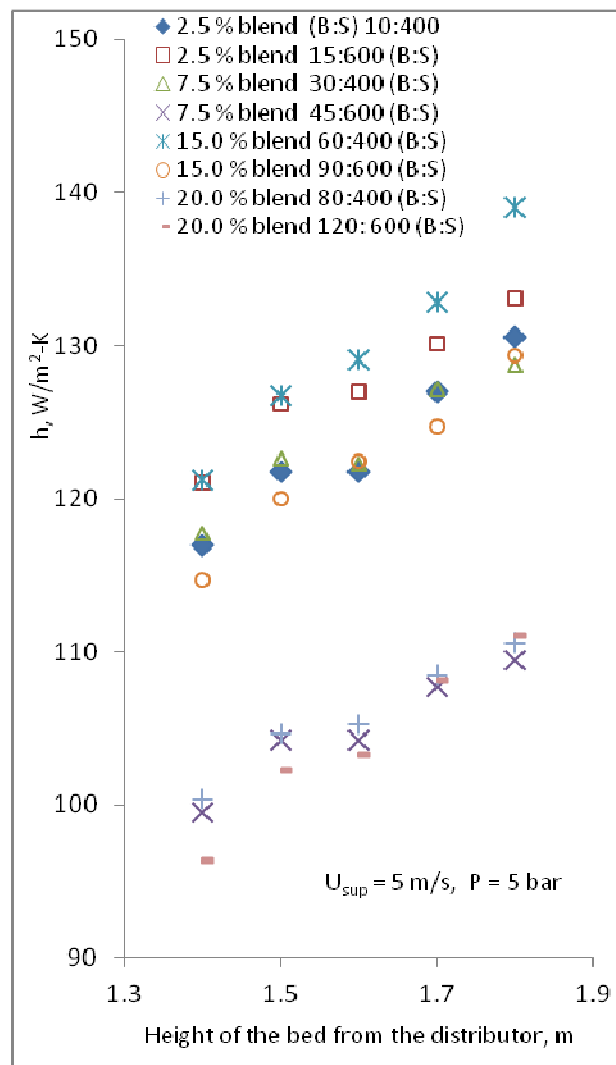


Fig. 14. Comparison of variation of heat transfer coefficient along the heat transfer probe.

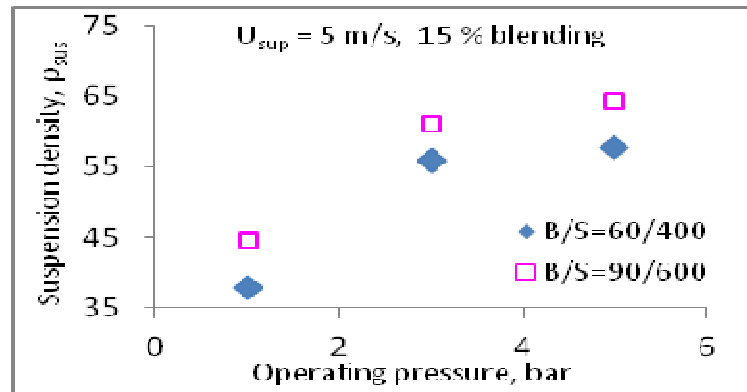


Fig. 15. Variation of suspension density at $U_{sup} = 5$ m/s.

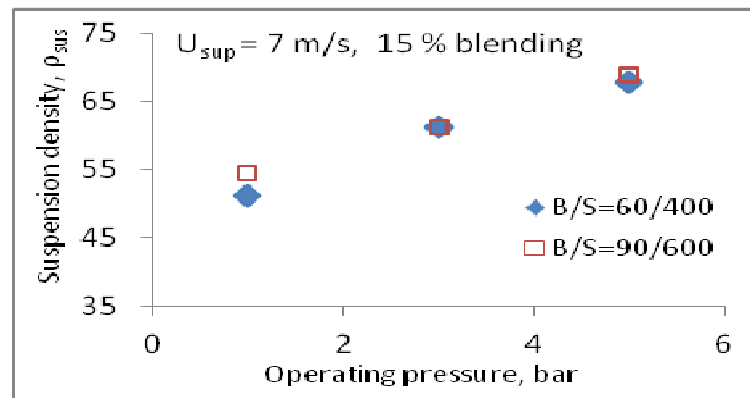


Fig. 16. Variation of suspension density at $U_{sup} = 7$ m/s.

Figure 14 show the variation of heat transfer coefficient along the heat transfer probe at the operating pressure of 5 bar and at the superficial velocity of 5 m/s. It is observed that, the heat transfer coefficient increases from the bottom to the top of the heat transfer probe. This is a representative figure for percentage blending of biomass in sand at varied pressure conditions. The similar variation of heat transfer coefficient without blending of biomass is demonstrated by Gupta and Nag [1].

The suspension density variation at a height of 1.57 m from the distributor with operating pressures at two different superficial velocities of 5 and 7 m/s are shown in Figures 15 and 16, respectively. The comparison is made at a percentage blending of 15 and at two different weight composition ratios. It has been observed that, the suspension density increases with the increase in operating pressure in both the weight composition ratios. However, the higher value of suspension density has

been observed at weight composition ratio (B/S) of 90 gm: 600 gm.

The comparison of radial variation of heat transfer coefficient at two different superficial velocities is presented in the Figures 17 through 20. These plots have been made at a distance of 1.6 m from the height of the distributor and at 2.5%, 15% and 20% sawdust blending. From these figures, it has been observed that, the heat transfer coefficient decreases from the wall to the core of the riser. This may be due to decrease in particle concentration from the wall to the core of the riser. It is also observed that with the increase in pressure heat transfer coefficient increases. This may be due to the increase in particle concentration with increase in pressure. At 20% biomass blending, heat transfer coefficient near to the wall of the riser is found be highest and at the core it is found to be lowest. This is probably due to the diffusion of particles from the core to the wall of the riser.

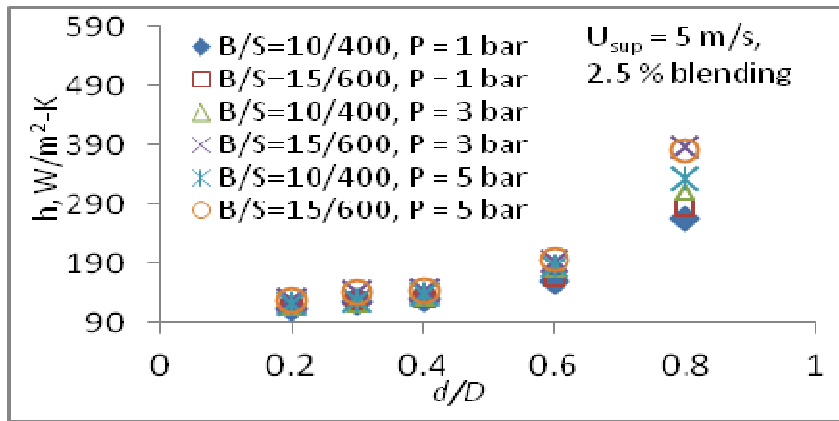


Fig. 17. Comparison of radial heat transfer coefficient at 2.5% blending.

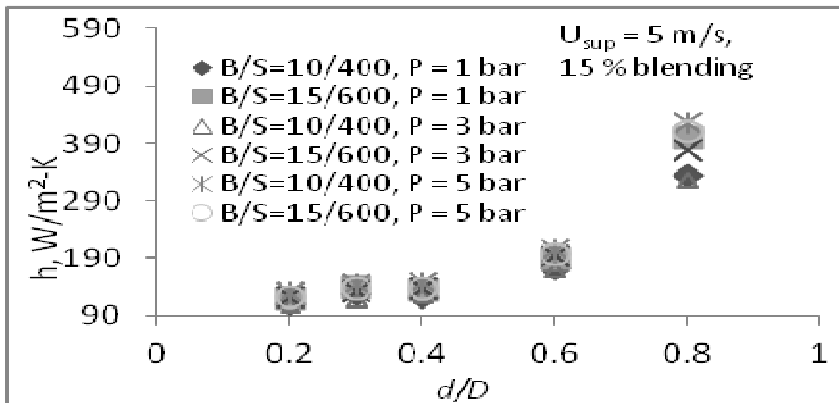


Fig. 18. Comparison of radial heat transfer coefficient at 15% blending.

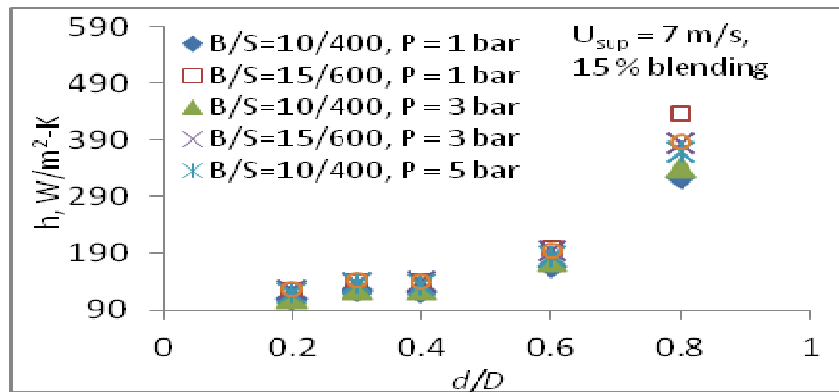


Fig. 19. Comparison of radial heat transfer coefficient at 15% blending.

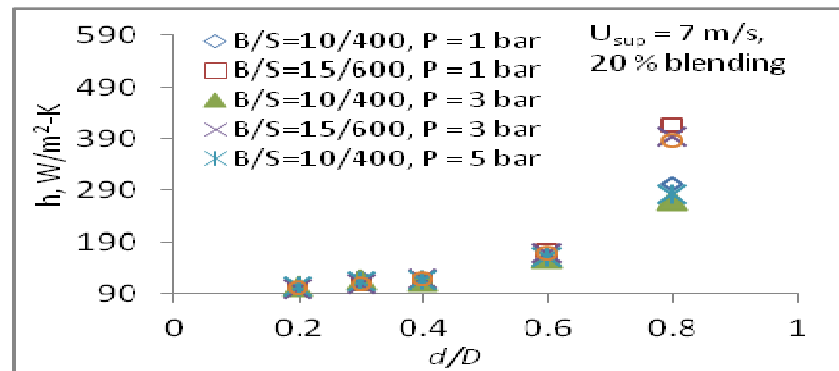


Fig. 20. Comparison of radial heat transfer coefficient at 20% blending.

Table 1. Solid circulation rate, G_s ($\text{kg m}^{-2}\text{s}^{-1}$) data with pressure.

P, bar	2.5% blend		7.5% blend		15.0% blend		20.0% blend	
	(B/S) 10:400	(B/S) 15:600	(B/S) 30:400	(B/S) 45:600	(B/S) 60:400	(B/S) 90:600	(B/S) 80:400	(B/S) 120: 600
$U_{\text{sup}} = 5 \text{ m/s}$								
1	0.816	1.381	0.946	1.072	0.773	0.912	0.205	0.0817
3	1.164	1.086	1.623	0.753	1.094	1.762	0.926	0.1388
5	0.9517	1.455	1.798	1.350	1.637	1.327	0.989	0.3033
$U_{\text{sup}} = 7 \text{ m/s}$								
1	1.296	1.406	1.565	1.261	1.137	1.451	1.064	0.1921
3	1.275	1.123	2.089	1.205	1.434	1.861	1.352	0.2609
5	1.093	1.455	2.012	1.260	1.389	1.650	1.332	0.3533

4. CONCLUSIONS

The present investigation may be concluded with the following observations

- The S-Shaped bed voidage profile along the height of the riser has been observed at all percentage blending and operating pressures.
- The suspension density increases with the increases in operating pressures.
- The axial heat transfer coefficient increases with an increase in operating pressure and superficial velocity.
- The radial heat transfer coefficient decreases from the wall (about $480 \text{ W/m}^2\text{-K}$) to the core ($93 \text{ W/m}^2\text{-K}$) of the riser in all the operating conditions.
- The solid circulation rate increases with an increase in operating pressures and superficial velocity, and it decreases with the increase in % blending of sawdust.
- More homogenous fluidization and uniform heat transfer coefficient has been observed with the increase in operating pressure. 7.5 - 15% sawdust blend in sand is observed to be optimum for obtaining higher heat transfer coefficient at both the sets of weight compositions.

NOMENCLATURE

A_B	Cross sectional area of the bed in m^2
A_D	Cross sectional area of downcomer in m^2
A_{htp}	Surface area of heat transfer probe in m^2
B	Weight composition of biomass particles
G_s	Solid circulation rate in $\text{kg m}^{-2}\text{s}^{-1}$
h	Heat transfer coefficient
Δh	difference of height in manometric fluid measured in cm of water column
I	Supply current
L_a	Solid accumulation height in m
L_m	Difference between two consecutive pressure taps
P	Operating pressure in bar
q	Heat flux
S	Weight composition of sand particles

t	Time to accumulate particular height after closing ball valve in sec
T_{bi}	Bed temperature in K
T_{bs}	Bulk surface temperature in K
U_{sup}	Superficial velocity in m/s
V	Supply Voltage
B/S	Biomass (sawdust) to sand ratio
ρ_g	Gas density in kg/m^3
ρ_s	Solid density in kg/m^3
ρ_{sus}	Suspension density in kg/m^3
ε	Bed voidage
ε_{mf}	Bed voidage at minimum fluidization

REFERENCES

- [1] Gupta A.V.S.S.K.S. and P.K. Nag. 2002. Bed-to-wall heat transfer behavior in a pressurized circulating fluidized bed. *International Journal of Heat and Mass Transfer* 45:3429-3436.
- [2] Basu P. and L. Cheng. 1996. Heat transfer in a pressurized circulating fluidized bed. *International Journal of Heat and Mass Transfer* 39(13):2711-2722.
- [3] Basu P., 2006. *Combustion and Gasification in Fluidized Beds*. Taylor & Francis Group (CRC Press), New York.
- [4] Basu P. and P.K. Nag. 1996. Heat transfer to walls of a circulating fluidized-bed furnace. *Chemical Engineering Science* 51(1):1-26.
- [5] Basu P. and P.K. Nag. 1987. An investigation into heat transfer in circulating fluidized beds. *International Journal of Heat and Mass Transfer* 30(11):2399-2409.
- [6] Grace J.R., 1986. Heat transfer in circulating fluidized beds. In: *Circulating Fluidized Bed Technology*, P. Basu (Ed.), Pergamon, Canada, pp.63-81.
- [7] Hartge E.U., Rensner D. and Werther J., 1988. Solid concentration and velocity patterns in circulating fluidized beds. In: *Circulating Fluidized Bed Technology II*, P. Basu and J.F. Large (Eds.), pp. 165-180. Pergamon Press, Oxford.

- [8] Horio M., Morishita K., Tachibana O., and Murata N., 1988. Solid distribution and movement in circulating fluidized beds. In: *Circulating Fluidized Bed Technology II*, P. Basu and J. F. Large (Eds.), pp. 147-154. Pergamon Press, Oxford.
- [9] Li J.J., Zhang H., Yang H.R., Wu Y.X., Lu J.F., and Yue G.X., Zhang. 2009. Hydrodynamic model with binary particle diameter to predict axial voidage profile in a CFB combustor. In *Proceedings of the 20th International Conference on Fluidized bed Combustion*, pp.768-773, China.
- [10] Yates J.G., 1997. Experimental observations of voidage in gas fluidized beds. In: *Non-Invasive Monitoring of Multiphase Flows*, J. Chaouki, F. Larachi, M.P. Duducovic (Eds.), pp.141-160. Elsevier, Amsterdam,
- [11] Tang J.T., and F. Engstrom. 1987. Technical assessment on the Ahlstrom pyroflow circulating and conventional bubbling fluidized bed combustion systems. In *Proceedings of the 9th International Conference on Fluidized Bed Combustion* (Edited by J.P. Mustonen), pp. 38-54. ASME, New York.
- [12] Schaub G., Reimert R., and Albrecht J., 1989. Investigation of emission rates from large scale CFB combustion plants. In *Proceedings of the 10th International Conference on Fluidized Bed Combustion*, A. Manaker (Ed.), pp. 685-691. ASME, New York.
- [13] Yue G., Lu J., Zhang H., Yong H., Zhang J., and Liu Q., 2005. Design theory of circulating fluidized boilers. In *Proceedings of the 18th International Conference on Fluidized Bed Combustion*, Jia, L., Ed., ASME, New York, paper: FBC 78134.
- [14] Li Y. and M. Kwauk. 1980. The dynamics of fast fluidization. In *Proceedings of the 3rd International Conference on Fluidized Bed Combustion*, J.R. Grace and J.M. Matsen (Eds.), August 3-8, pp. 539-544. Henniker, New Hampshire.
- [15] Kunii D. and O. Levenspiel. 1991. *Fluidization Engineering*, Butterworth-Heinemann, USA.
- [16] Andersson B.A. and B. Leckner. 1992. Experimental methods of estimating heat transfer in circulating fluidized bed. *International Journal of Heat Mass Transfer* 35:3353-3362.
- [17] Brereton C.M.H. and L. Stromberg. 1986. Some aspects of fluid dynamic behavior of fast fluidized beds, In *Circulating Fluidized Bed Technology*, P. Basu (Eds.), pp.133-144. Pergamon Press, Toronto.
- [18] Yates J.G., 1996. Effects of Temperature and Pressure on Gas-Solid Fluidization. *Chemical Engineering Science* 51(2):167-205.
- [19] Wu R., Lim C.J., Chauki J., and Grace J.R., 1987. Heat transfer from a circulating fluidized bed to membrane water wall cooling surfaces. *A.I.Ch.E.Journal* 33:1888-1893.
- [20] Ebert T.A., Glicksman L.R., and Lints M., 1993. Determination of particle and gas convective heat transfer component in circulating fluidized bed. *Chemical Engineering Science* 48: 2179-2188.
- [21] Nag P.K. and Ali Moral M.N., 1990. Effect of probe size on heat transfer at the wall in circulating fluidized beds. *International Journal of Energy Research* 14:965-974.
- [22] Mahalingam M. and A.K. Kolar. 1991. Heat transfer model for the membrane wall of a high temperature circulating fluidized bed. In *Circulating Fluidized Bed Technology III*, P. Basu, M. Horio, and M. Hasatani (Eds.), pp. 239-246. Pergamon Press, Oxford.
- [23] Divilio R.J. and T.J. Boyd. 1994. Practical implications of the effect of solids suspension density on heat transfer in large scale CFB boilers. In *Circulating Fluidized Bed Technology IV*, A. Avidan (Ed.), pp. 334-339. AIChE, New York.
- [24] Glicksman L., 1988. Circulating fluidized bed heat transfer. In *Circulating Fluidized Bed Technology II* P. Basu and J.F. Large (Eds.), pp. 13-29. Pergamon Press, Oxford.
- [25] Oka S.N. and E.J. Anthony. 2004. *Fluidized Bed Combustion*, Marcel Dekker Inc (CRC Press), New York.